Journal of Alzheimer's Disease 29 (2012) 783–791
DOI 10.3233/JAD-2012-111880
IOS Press

Impaired Neuronal Insulin Signaling Precedes $A\beta_{42}$ Accumulation in Female AβPPsw/PS1ΔE9 Mice

Li-Min Chua[a], Mei-Li Lim[a], Pey-Rou Chong[a], Ze Ping Hu[a,1], Nam Sang Cheung[b] and Boon-Seng Wong[a,*]
[a]*Department of Physiology, Yong Loo Lin School of Medicine, National University of Singapore, Singapore*
[b]*School of Life and Environmental Sciences, Faculty of Science and Technology, Deakin University, Victoria, Australia*

Handling Associate Editor: Xiongwei Zhu

Accepted 3 January 2012

Abstract. Reduced glucose utilization is likely to precede the onset of cognitive deficits in Alzheimer's disease (AD). Similar aberrant glucose metabolism can also be detected in the brain of several AD mouse models. Although the cause of this metabolic defect is not well understood, it could be related to impaired insulin signaling that is increasingly being reported in AD brain. However, the temporal relationship between insulin impairment and amyloid-β (Aβ) biogenesis is unclear. In this study using female AβPPsw/PS1ΔE9 mice, we found that the level of $A\beta_{40}$ was fairly constant in 6- to 15-month-old brains, whereas $A\beta_{42}$ was only significantly increased in the 15-month-old brain. In contrast, increased levels of IRβ, IGF-1R, IRS1, and IRS-2, along with reduced glucose and insulin content, were detected earlier in the 12-month-old brains of AβPPsw/PS1ΔE9 mice. The reduction in brain glucose content was accompanied by increased GLUT3 and GLUT4 levels. Importantly, these changes precede the significant upregulation of $A\beta_{42}$ level in the 15-month-old brain. Interestingly, reduction in the p85 subunit of PI3K was only apparent in the 15-month-old AβPPsw/PS1ΔE9 mouse brain. Furthermore, the expression profile of IRβ, IRS-2, and p85/PI3K in AβPPsw/PS1ΔE9 was distinct in wild-type mice of a similar age. Although the exact mechanisms underlining this connection remain unclear, our results suggest a possible early role for insulin signaling impairment leading to amyloid accumulation in AβPPsw/PS1ΔE9 mice.

Keywords: Alzheimer's disease, amyloid, glucose transporter, insulin signaling, neurodegeneration

INTRODUCTION

Brain imaging studies have demonstrated deficits in glucose utilization in Alzheimer's disease (AD) [1, 2], and this hypometabolism of glucose may precede the onset of cognitive deficits [3–5]. A similar reduction in glucose utilization was also detected in the brain of several AD mouse models [6–8]. However, the cause of this defect is not well understood. Despite that, it is possible that impaired mitochondrial function [1, 9] or defective glucose transportation [10] might have contributed to this observation.

Glucose metabolism in the peripheral is known to be regulated mainly by insulin signaling [11], but little is known about the role of insulin in the brain [12]. An increasing number of epidemiological studies have suggested a connection between diabetes and AD [13, 14] and recent reports have also documented aberrant insulin signaling in AD brain [15–18]. These reports have observed a significant reduction in several key

[1]Current address: Biological Sciences Division, Pacific Northwest National Laboratory, Richland WA, USA.

*Correspondence to: Dr. Boon-Seng Wong, Department of Physiology, Yong Loo Lin School of Medicine, National University of Singapore, Singapore. Tel.: +65 6516 7617; Fax: +65 6777 3271; E-mail: bswong@nus.edu.sg.

ISSN 1387-2877/12/$27.50

substrate adaptor proteins involved in insulin signaling in the AD brain [17, 19, 20]. However, the temporal relationship between insulin impairment and the accumulation of amyloid-β (Aβ) peptide (principally $A\beta_{40}$ and $A\beta_{42}$) with changes in glucose utilization is unknown.

In this manuscript, we used female AβPPsw/PS1ΔE9 mice [21] to document the change in brain $A\beta_{40}$ and $A\beta_{42}$ levels with the expression level of key insulin signaling proteins and the glucose and insulin content in 6-, 12-, and 15-month-old brains. While significant elevation of $A\beta_{42}$ level was only detected in the 15-month-old brain, reduction in insulin and glucose content occurred earlier in the 12-month-old brain. This early reduction in brain insulin and glucose level was also associated with a significant upregulation of insulin-like growth factor 1 receptor (IGF-1R) and insulin receptor β (IRβ) together with two key substrate adaptor proteins; insulin receptor substrate 1 and 2 (IRS-1 and IRS-2). However, the apparent increases in IRS-1 and IRS-2 levels were only detected in the 12-month-old brain but not the 15-month-old brain of AβPPsw/PS1ΔE9. In contrast, a reduction in the regulatory p85 subunit of phosphatidylinositol 3-kinase (p85/PI3K) was only detected in 15-month-old AβPPsw/PS1ΔE9 mouse brain. Nevertheless, the down-regulation of PI3K did not lead to a detectable change in Akt phosphorylation with respect to total Akt. In addition, the reduced brain glucose content was also accompanied by increased glucose transporters 3 and 4 (GLUT3 and GLUT4) level. Taken together, the change in the expression level of key insulin signaling proteins preceded the significant increase in brain $A\beta_{42}$ level in AβPPsw/PS1ΔE9 mice. This early perturbation in brain insulin signaling was accompanied by reduced glucose and insulin content.

MATERIALS AND METHODS

Animals

The experimental protocol (protocol #009/06) involving the maintenance and euthanasia of laboratory mice was in accordance with guidelines approved by the Institutional Animal Care and Use Committees (IACUC) at the National University of Singapore. Briefly, mice were anesthetized and blood was collected by cardiac puncture before harvesting their brains. Mice used in this study were hemizygous mutant B6C3-Tg(AβPPsw/PS1ΔE9)85Dbo/J mice [21] from The Jackson Laboratory (JAX004462), with their wild-type littermates used as controls. The mutant mice express AβPP harboring the Swedish mutation (K594M/N595 L) and the presenilin-1 gene in which exon 9 is deleted (PS1ΔE9). Female transgenic and wild-type mice of 3 ages; 6, 12, and 15 months were used respectively. Four brains and plasma of four animals ($n = 4$) from each time point in the animal groups were used in all immunochemical and biochemical analysis, whereas two brains ($n = 2$) from each time point in the animal groups were used in all immunoblotting.

Preparation of brain homogenates

Brain tissues, snapped frozen in liquid nitrogen when harvested, were used for lysis of the tissue samples. The wet weight of the tissues (in mg) was determined using an electronic balance and 1× cell lysis buffer (Cell Signaling Technology) with protease inhibitor tablet (Roche) was added at 20% (w/v) ratio. Lysates were then homogenized using a PowerGen homogenizer (ThermoFisher Scientific) at 3 pulses of 20 s each, with a 10 s interval on ice in between to reduce excessive heat that was generated during homogenization. For subsequent downstream applications, tissue lysates were further diluted 10 times in cell lysis buffer and sonicated briefly to ensure complete lysis. The crude brain homogenates were stored at −80°C and protein concentrations were determined by spectrophotometry using the Pierce™ MicroBCA assay kit (ThermoFisher Scientific).

Preparation of blood plasma

Whole blood was collected in tubes containing anticoagulant before the samples were fractionated by centrifugation at 3000 × g for 10 min to obtain blood plasma. The plasma was extracted by use of a transfer pipette and stored frozen at −80°C.

Immunoblot and densitometric analysis

Fifty micrograms (μg) of total brain lysate samples were boiled at 95°C for 10 min in gel-loading buffer to denature the proteins followed by electrophoretic separation on 7.5% Tris-glycine polyacrylamide gels [22]. The separated proteins were transferred onto a nitrocellulose membrane, probed with the respective primary antibodies and exposed to horseradish peroxidase (HRP)-conjugated secondary antibodies. The reactive protein bands were visualized by chemiluminescence using the SuperSignal® West Dura Substrate (Pierce) system. All the blots were

digitally developed using the Image Station 4000R (CareStream Health Inc.). Pre-stained Precision Plus™protein standards (Bio-Rad) were used to estimate the apparent molecular weight of the protein bands. Immunoblotting of β-actin using a rabbit polyclonal antibody that binds to the C-terminal of β-actin (Sigma) was included in all western blot analysis to ensure comparable protein loading. The primary antibodies used include anti-GLUT3 (Millipore, Cat# AB1344), anti-GLUT4 (Cell Signaling Technology, Cat# 2213), anti-IRβ (Cell Signaling Technology, Cat# 3020), anti-IGF1R (Cell Signaling Technology, Cat# 3018), anti-IRS1 (Cell Signaling Technology, Cat# 2382), anti-IRS2 (Cell Signaling Technology, Cat# 4502), anti-PI3K (Cell Signaling Technology, Cat# 4292), anti-Akt (Cell Signaling Technology, Cat# 4691), and anti-pAkt(S473) (Cell Signaling Technology, Cat# 4060). All immunoblots were re-probe for up to 3 different protein targets including β-actin. The re-probing was performed by stripping the initial antibody binding using the Restore Western Blot Stripping Buffer (Pierce) according to manufacturer's instruction, washed and incubating the stripped membrane with the new primary antibody. Densitometry analysis was performed [22] by measuring the optical densities of the targeted protein bands relative to the endogenous β-actin level. For protein phosphorylation, the optical densities of the phosphorylated protein bands were measured relative to the targeted total protein level. The analysis was performed using the NIH ImageJ software.

Aβ ELISA assay

Aβ quantification was performed using the Human $A\beta_{40}$ (Cat# 27714) and Human $A\beta_{42}$ (Cat# 27712) assay kits (Immuno-Biological Laboratories Co, Japan) according to manufacturer's instructions. Before the assay, mouse brain lysates were further homogenized with 5 M guanidine HCl/50 mM Tris-HCl/pH 8 and diluted 500-fold before incubating the mixtures for 3 hours at room temperature with vigorous shaking at 450 rpm. The samples were further diluted 100 times in the provided EIA buffer before they were used for Aβ quantification. The absorbance readings were taken at 450 nm.

Glucose assay

Total brain glucose content was measured using the amplex red glucose assay kit (Life Technologies) following the instructions provided by the manufacturer. Briefly a serial dilution of brain lysates was performed using the assay buffer provided before an equal volume of amplex red working reagent was added. For the analysis of plasma glucose content, samples were mixed with equal volume of the amplex red working reagent. For both assays, the reaction mixture was incubated for 30 min at room temperature in the dark before fluorescence values were read at an excitation wavelength of 535 nm and an emission wavelength of 590 nm. A series of glucose standards were prepared and run alongside the samples.

Insulin assay

Brain insulin content was measured using the sandwich ELISA mouse insulin assay system (Millipore) following the instructions provided by the manufacturer. Briefly, brain lysates were added to a microtitre plate well pre-coated with anti-insulin antibody. After incubation and washing, a biotinylated anti-insulin antibody was added. This biotinylated antibody reacts against a distinctive epitope to that of the coated anti-insulin. Following that, immnoreactivity was determined by measuring the absorbance at 450 nm.

Statistical analysis

Significant differences were analyzed using two-tailed Student's *T*-test. A p value of < 0.05 is considered significant.

RESULTS

$A\beta_{40}$ and $A\beta_{42}$ levels in the AβPPsw/PS1ΔE9 mouse brain

$A\beta_{40}$ and $A\beta_{42}$ are two widely characterized Aβ peptides in AβPP transgenic mice [23]. In this study, we found that the level of $A\beta_{42}$ was higher than $A\beta_{40}$ in the guanidine hydrochloride-treated brain tissues from 6- and 12-month-old AβPPsw/PS1ΔE9 mice (Fig. 1). However, a significant elevation in $A\beta_{42}$ level compared to $A\beta_{40}$ level was only apparent in the 15-month old transgenic mouse brain.

Brain glucose content and the expression of glucose transporters

Reduced glucose metabolism is well documented in AD [1, 2] and is believed to be an early pathologi-

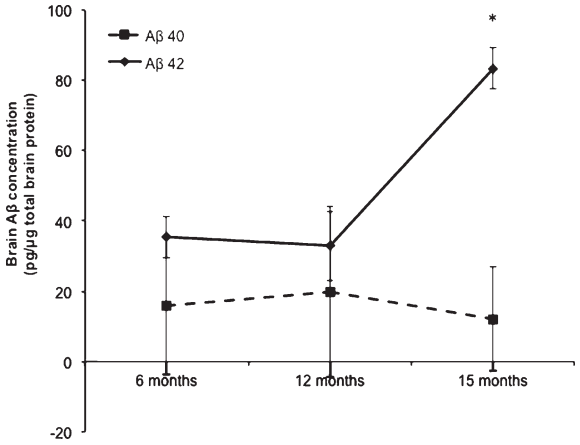

Fig. 1. $A\beta_{40}$ and $A\beta_{42}$ levels in the aging AβPPswe/PS1dE9 mouse brain. Cerebral steady state levels of $A\beta_{40}$ (dotted line) and $A\beta_{42}$ (full line) were quantified by sandwich ELISA in guanidine hydrochloride-treated brain lysates from AβPPswe/PS1dE9 mice at 6, 12, and 15 months old. Each value represents the mean ± SEM of duplicate assays for individual mouse brain sample ($n = 4$ at each time point for each mouse line). $A\beta_{42}$ level was significantly elevated as compared to $A\beta_{40}$ level in the brain of 15-month-old AβPPswe/PS1dE9 mice ($^*p < 0.05$ using Student's t-test).

cal event preceding Aβ accumulation [3–5]. As shown in Fig. 2a, a significant reduction of >1 fold in brain glucose content was detected in the 12- and 15-month-old AβPPsw/PS1ΔE9 mouse brain as compared to wild-type mouse brain. This change occurred before the significant upregulation of $A\beta_{42}$ in 15-month-old transgenic mice (Fig. 1). In contrast, we did not detect any significant change in the plasma glucose content from the AβPPsw/PS1ΔE9 mice as compared to the wild-type mice (Fig. 2b). For both studies, in order to ensure that the glucose reading does not include trace elements in the assay buffers, we included controls containing only the respective buffers used in this assay. The fluorescence readings from the controls were subtracted from all readings for the brain lysates.

We next examined the protein expression of two common glucose transporters (GLUT) found in the brain; GLUT3 and GLUT4. In wild-type mice, there was an upregulation of GLUT3 between 6 to 15 months (Fig. 2b). In the AβPPsw/PS1ΔE9 mouse brain, however, an increased GLUT3 level was only observed in 12-month-old mice, which remained unchanged in the 15-month-old mice (Fig. 2b).

In contrast, upregulation of GLUT4 could only be detected in the 15-month-old wild-type mouse brain. But in AβPPsw/PS1ΔE9, an apparent increase in GLUT4 level was observed in the 12-month-old mouse brain, which remained unchanged in the 15-month-old mouse brain (Fig. 2b).

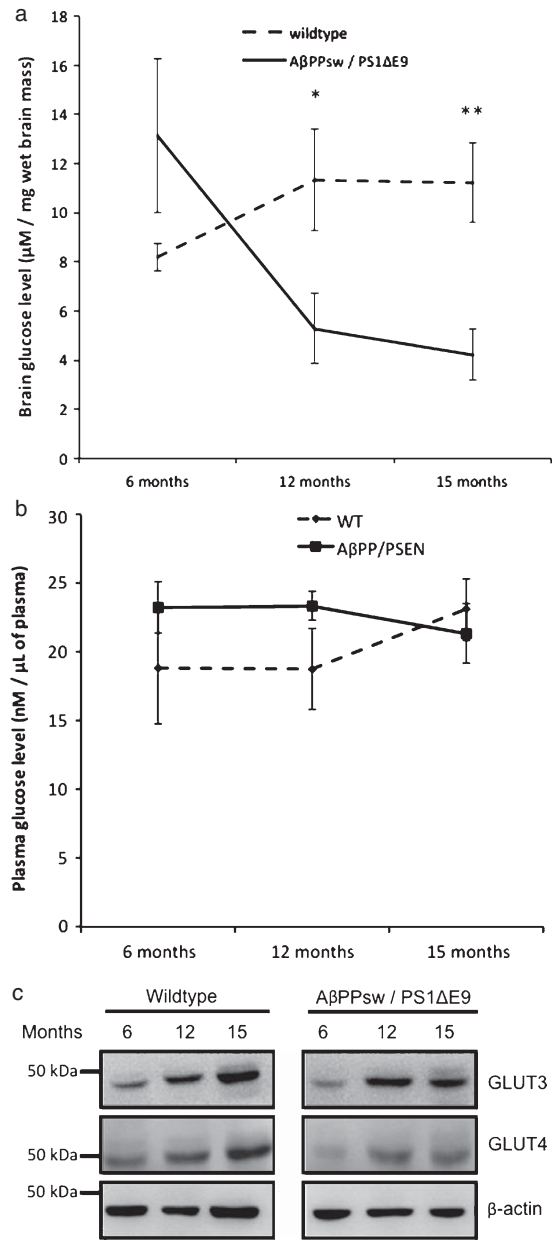

Fig. 2. Analysis of total brain and plasma glucose content, and mouse brain glucose transporter expression. (a) Total brain and (b) plasma glucose content from 6-, 12-, and 15-month-old wild-type and AβPPsw/PS1ΔE9 mice. Each value represents the mean ± SEM of duplicate assays for individual mouse (a) brain or (b) plasma sample ($n = 4$ at each time point for each mouse line). Only brain glucose was significantly reduced in AβPPsw/PS1ΔE9 mice as compared to wild-type mice at 12 and 15 months old ($^*p < 0.05$; $^{**}p < 0.01$ using Student's t-test). (c) Western blot analysis of ~48 kDa glucose transporter 3 (GLUT3) and ~50 kDa glucose transporter 4 (GLUT4) in the brain of 6-, 12-, and 15-month-old wild-type and AβPPsw/PS1ΔE9 mice. β-actin (~42 kDa) was immunoblotted to ensure similar gel loading of the starting material in each sample. The immunoblot is a representation of two animal brain samples analyzed in each age group from each mouse line ($n = 2$).

Brain insulin content and insulin receptor expression

Defects in brain insulin signaling are well documented in AD [17, 19], but the temporal onset of this impairment is unclear. As shown in Fig. 3a, a significant reduction of >4 folds in brain insulin content was detected in 12- and 15-month-old AβPPsw/PS1ΔE9 mice as compared to similarly aged wild-type mice. To ensure that the insulin reading does not include trace amounts that may be present in the assay buffers, we included controls containing only the assay reagents. Subsequently, the absorbance readings from the controls were subtracted from all readings for the brain lysates. We are unable to measure plasma insulin level due to insufficient transgenic mouse blood samples.

We next examined the protein level of insulin receptor β-subunit (IRβ) in wild-type and AβPPsw/PS1ΔE9 mice. In wild-type mice, an apparent increase in IRβ level was observed in the 12-month-old mouse brain (Fig. 3b). However, this was reduced in the 15-month-old brain to a level comparable to that in the 6-month-old brain (Fig. 3b). In the AβPPsw/PS1ΔE9 mice, an apparent increase in IRβ level was also observed in the 12-month-old brain, but appeared to remain elevated in the 15-month-old mouse brain (Fig. 3b).

A similar increment pattern for IGF-1 receptor (IGF-1R) expression level was also observed in the wild-type and AβPPsw/PS1ΔE9 mouse brains (Fig. 3b). In wild-type mice, there was an apparent increase in IGF-1R levels in the 12-month-old brain followed by a subsequent reduction of IGF-1R in the 15-month-old brain. For the AβPPsw/PS1ΔE9 mice, the apparent increase in IRβ level in the 12-month-old brain remained elevated in the 15-month-old mouse brain (Fig. 3b).

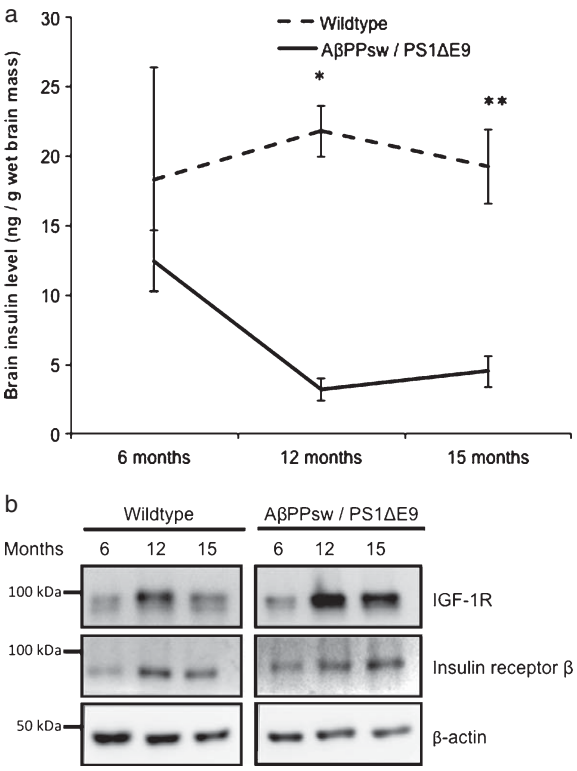

Fig. 3. Analysis of brain insulin content and insulin receptor expression in the aging mouse brain. (a) ELISA analysis of insulin content in brain lysates from 6-, 12-, and 15-month-old wild-type and AβPPsw/PS1ΔE9 mice. Each value represents the mean ± SEM of duplicate assays for individual mouse brain sample ($n = 4$ at each time point for each mouse line). Brain insulin content was significantly reduced in 12- and 15-month-old AβPPsw/PS1ΔE9 mice as compared to respective age in wild-type mice ($^*p < 0.001$; $^{**}p < 0.01$ using Student's *t*-test). (b) Western blot analysis of ~95 kDa insulin receptor β-subunit and ~95 kDa IGF1 receptor (IGF1R) levels in the brain of 6-, 12-, and 15-month-old wild-type and AβPPsw/PS1ΔE9 mice. β-actin (~42 kDa) was immunoblotted to ensure similar gel loading of the starting material in each sample. The immunoblot is a representation of two animal brain samples analyzed in each age group from each mouse line ($n = 2$).

Insulin signaling protein expression in the aging mouse brain

We next examined the expression of major proteins involved in the insulin signaling pathway. As shown in Fig. 4a and b, densitometric analysis showed insulin receptor substrate 1 (IRS1) level in AβPPsw/PS1ΔE9 mice peaked in the 12 month-old mouse brain, but was reduced in the 15-month-old brain. While IRS1 level was comparable in 12-month-old wild-type and AβPPsw/PS1ΔE9 mouse brains, it is lower in 12- and 15-month-old wild-type mouse brains as compared to similar aged AβPPsw/PS1ΔE9 mouse brains.

A similar expression profile was also observed for IRS2 level in AβPPsw/PS1ΔE9 mouse brain (Fig. 4a and c). IRS2 level in AβPPsw/PS1ΔE9 mice peaked in the 12 month-old mouse brain, but was reduced in the 15-month-old brain to a level comparable to the 6-month-old brain. In wild-type mice, a slight reduction in IRS2 level was observed in the 15-month-old brain.

Interestingly, there was no apparent change in the p85 subunit of the phosphatidylinositol 3-kinase (p85/PI3K) level in the aging brains of wild-type mice. However, densitometric analysis showed that the p85/PI3K level was reduced in 15-month-old AβPPsw/PS1ΔE9 mouse brain (Fig. 4d).

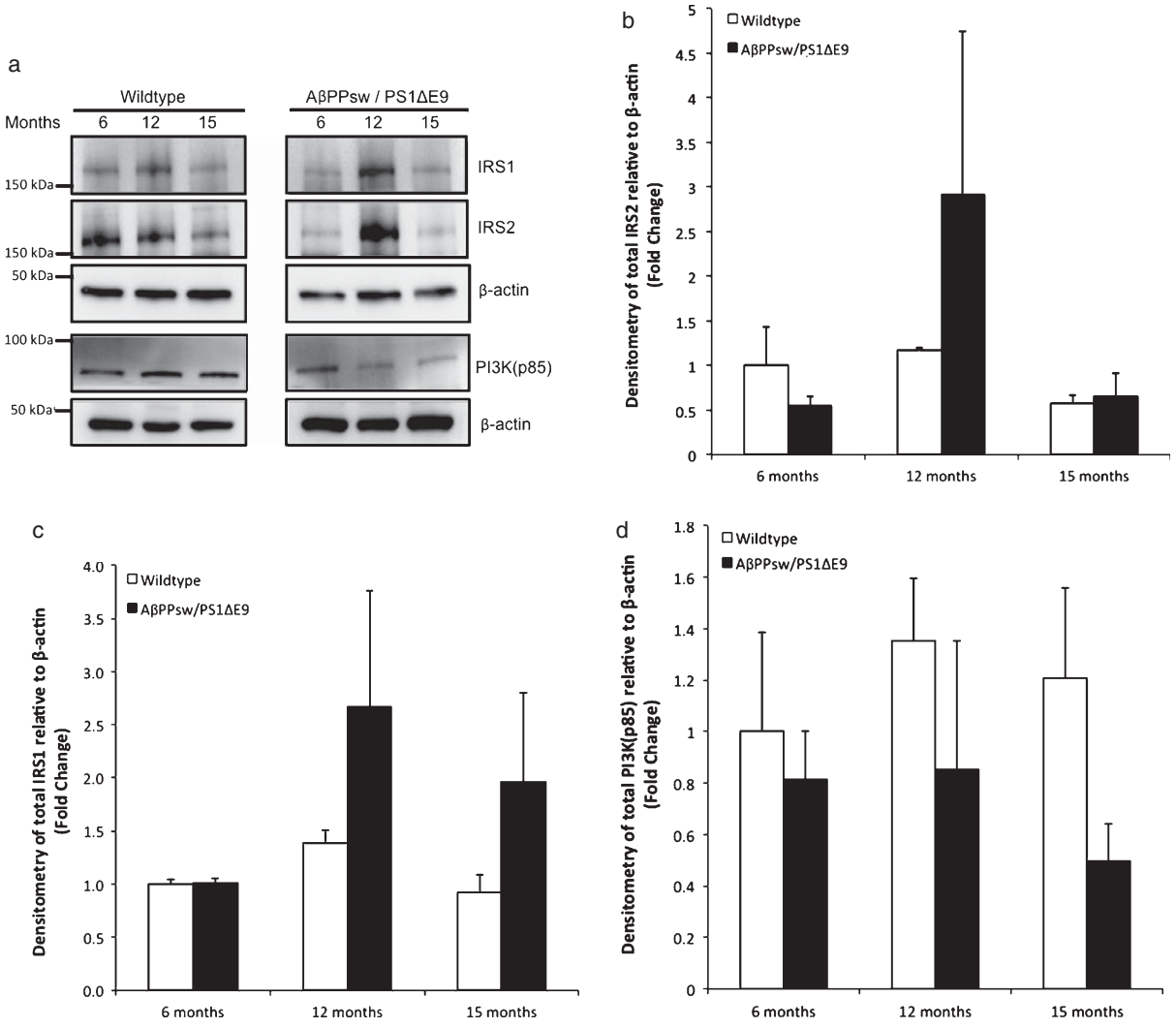

Fig. 4. Insulin signaling protein expression in the aging mouse brain. (a) Western blot analysis of ∼180 kDa insulin receptor substrate-1 (IRS-1), ∼185 kDa insulin receptor substrate-2 (IRS-2), the p85 subunit (∼85 kDa) of phosphatidylinositol 3-kinase (p85/PI3K) levels in the brain of 6-, 12-, and 15-month-old wild-type and AβPPswPS1dE9 mice. β-actin (∼42 kDa) was immunoblotted to ensure similar gel loading of the starting material in each sample. The immunoblot is a representation of two animal brain samples analyzed in each age group from each mouse line ($n = 2$). Densitometry analysis of (b) IRS1, (c) IRS2 and (d) p85/PI3K relative to β-actin in 6-, 12-, and 15-month-old wild-type (white bar) and AβPPsw/PS1ΔE9 (black bar). Analysis was performed using the NIH ImageJ software and values obtained for individual protein target for each brain sample were normalized against β-actin from the same brain sample. Each value represents the mean ± SEM for individual mouse brain sample ($n = 2$ at each time point for each mouse line).

Akt expression and phosphorylation in the aging mouse brain

In wild-type mice, total Akt expression was upregulated in the 12-month-old brain but significantly reduced in the 15-month-old brain (Fig. 5a). This was in contrast to what was observed in the AβPPsw/PS1ΔE9 mice, where total Akt expression was not significantly altered (Fig. 5a).

We next decided to examine the Akt phosphorylation status in the mouse brains (Fig. 5a and b). Densitometry analysis of phosphorylated Akt (S473) relative to total Akt in wild-type mice indicated an upregulation in 15-month-old brain. In contrast, the optical ratio of pAkt/Akt was relatively unchanged in AβPPsw/PS1ΔE9 mouse brain.

DISCUSSION

Brain imaging studies have shown that impaired glucose utilization in AD [1, 2] precedes the onset of

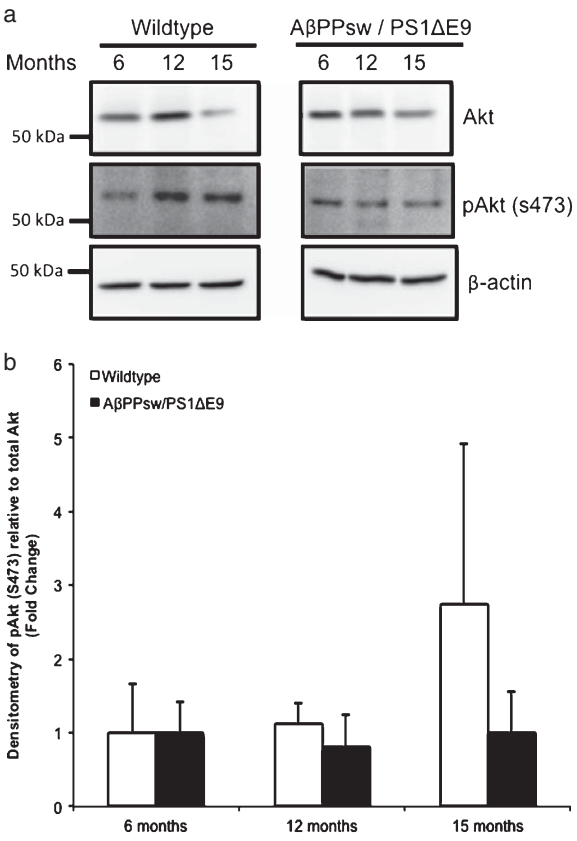

Fig. 5. Akt expression and phosphorylation in the aging mouse brain. (a) Western blot analysis of ∼60 kDa total Akt and ∼60 kDa phosphorylated Akt (ser473) levels in the brain of wild-type and AβPPsw/PS1ΔE9 mice at 6, 12, and 15 months old. β-actin (∼42 kDa) was immunoblotted to ensure similar gel loading of the starting material in each sample. The immunoblot is a representation of two animal brain samples analyzed in each age group from each mouse line ($n = 2$). (b) Densitometry analysis of phosphorylated Akt (ser473) over total Akt in 6-, 12-, and 15-month-old wild-type (white bar) and AβPPsw/PS1ΔE9 (black bar). Analysis was performed using the NIH ImageJ software and values obtained for phosphorylated Akt (ser473) for each brain sample were normalized against the total Akt from the same brain sample. Each value represents the mean ± SEM for individual mouse brain sample ($n = 2$ at each time point for each mouse line).

cognitive deficits [3–5]. A similar reduction in glucose utilization was also detected in the brain of several AD mouse models [6–8]. However, the cause of this defect is not well understood.

One possible explanation for the defect in glucose utilization in AD could be changes in the regulation of glucose metabolism caused by insulin signaling dysfunction [11]. Since impaired insulin signaling is increasingly observed in the AD brain [15–20], it is likely that brain glucose metabolism defects could be associated with this impairment in AD brain. Therefore, we used female AβPPsw/PS1ΔE9 mice in this study to investigate the temporal relationship between insulin signaling impairment and the accumulation of Aβ peptide (principally $A\beta_{40}$ and $A\beta_{42}$) with changes in brain glucose and insulin content. Female mice were chosen for this study as mice of the same gender from other mutant AβPP transgenic mouse strains have been reported to produce a significantly higher amyloid burden and subsequent plaque deposition than their male counterparts [23].

In female AβPPsw/PS1ΔE9 mice [21], we show for the first time that increased levels of IRβ, IGF-1R, IRS1, and IRS-2 along with reduced glucose and insulin content is detectable in the 12-month-old brain. This reduction in brain glucose content was accompanied by increased GLUT3 and GLUT4 levels. Notably, these changes precede the significant upregulation of $A\beta_{42}$ level in the 15-month-old brain. This late change in $A\beta_{42}$ level also coincides with reduction in p85/PI3K expression in the 15-month-old transgenic mice. The expression profile of IRβ, IRS-2, and PI3K in AβPPsw/PS1ΔE9 mice was also distinct from wild-type mice of a similar age.

Unlike other studies using similar mouse lines [6, 21], which documented the amyloid deposition histologically, we began by performing a temporal measurement of $A\beta_{40}$ and $A\beta_{42}$ levels in the 6-, 12-, and 15-month-old brain of AβPPsw/PS1ΔE9 mice. We found that $A\beta_{40}$ levels were fairly constant in the aging AβPPsw/PS1ΔE9 mouse brain and $A\beta_{42}$ was only significantly increased in the 15-month-old brain. However, an earlier study is able to detect significant plaque pathology in the cortex and hippocampus in 9-month-old AβPPsw/PS1ΔE9 mice [24].

We next examined the brain glucose content in the AβPPsw/PS1ΔE9 mice. An earlier study had reported a reduction in basal brain glucose levels in similar mouse line at ∼10 months old [6]. In our study, we detected this reduction in glucose level in the 12- and 15-month-old brains but not in the younger 6-month-old brain, as compared to wild-type mouse brains of similar age (Fig. 2a). However, we did not detect any significant change in plasma glucose from both mouse strains (Fig. 2b). This decrease in brain glucose was accompanied by a detectable increase in GLUT3 and GLUT4 levels in the 12-month-old AβPPsw/PS1ΔE9 mouse brain (Fig. 2c). However, other studies have reported a decrease in the expression of other GLUTs in the brain, such as GLUT1 in AβPPsw/PS1ΔE9 mice [10]. Unlike the brain-specific GLUT3, GLUT1 and GLUT4 can be detected in the brain and other peripheral tissues [25]. Thus, it is likely

that the expression of GLUTs varies even in the same tissue type.

In contrast to AβPPsw/PS1ΔE9 mice, GLUT3 level was gradually increased from 6- to 15-month-old brain, whereas GLUT4 was only upregulated in the 15-month-old brain of wild-type mice (Fig. 2c). The discrepancy between low glucose level and increased GLUT expression in AβPPsw/PS1ΔE9 mice suggests a possible decrease in GLUT activity levels, which would have caused less glucose uptake into the brain despite the high protein expression level. In addition, our finding of an increased amyloid deposition coupled with high GLUT3 levels and low brain glucose content is in line with previous study showing high Aβ level in neurons is associated with decreased glucose uptake and increased GLUT3 transcription [26].

Similar to brain glucose, brain insulin content was also significantly reduced in 12- and 15-month-old AβPPsw/PS1ΔE9 mice as compared to wild-type mice of similar ages (Fig. 3a). However, the expression level of IRβ and IGF-1R was elevated in the 12- and 15-month-old brain of the AβPP/PS1 transgenic mice (Fig. 3b). This is in agreement with another study showing increased IGF-1R level in AD temporal cortex [19]. As such, it is likely that the increase in IGF-1R and IRβ is a compensatory response toward declining brain insulin levels in the AβPPsw/PS1ΔE9 mice. Although a similar increase in IRβ and IGF-1R was also detected in the 12-month-old wild-type mouse brain, both protein levels were reduced in the older 15-month-old brain (Fig. 3b).

Further, this early reduction in brain insulin and glucose level was also associated with a significant upregulation of two key substrate adaptor proteins; IRS-1 and IRS-2 (Fig. 4). However, the apparent increase in IRS-1 and IRS-2 level was detected in the 12-month-old but reduced in the 15-month-old brain. Since Aβ has been reported to target IRS-1 for degradation via JNK activation [27], the higher $A\beta_{42}$ level in the 15-month-old brain could have facilitate IRS-1 degradation. However, it is unclear whether similar mechanism also underlies IRS-2 reduction. In wild-type mouse brain, IRS-1 and IRS-2 levels were relatively stable in the mouse brain as compared to AβPPsw/PS1ΔE9 mice (Fig. 4). This observation suggests that high amyloid burden in the 15-month-old mouse brain could lead to IRS degradation. The consistently high IRS level could also indicate a compensatory response toward declining brain insulin level, as the peak in protein level occurred when brain insulin level registered a steep decline from the 6- to 12-month-old AβPPsw/PS1ΔE9 mice.

In contrast, a reduction in the regulatory p85 subunit of PI3K was detected in the 15-month-old brain of AβPPsw/PS1ΔE9 but not wild-type mice (Fig. 4a and d). This reduction coincides with the accumulation of $A\beta_{42}$. In fact, our observation parallels an earlier report showing reduced p85/PI3K in AD brain tissues [28]. Furthermore, our study has expanded this observation by showing that p85 level varies with the increasing amyloid deposition in the transgenic mouse brain. This could affect the recruitment of the p110 catalytic subunit of PI3K for subsequent activation of insulin signaling. Further, studies have also shown p85 is able to negatively regulate insulin signaling [29]. Hence, it is possible that decreasing p85 level in the transgenic mouse brain could affect insulin sensitivity and thus brain glucose level.

However, the diminution in p85/PI3K level did not lead to a detectable change in Akt phosphorylation with respect to total Akt (Fig. 5). This was in contrast to the increased Akt phosphorylation observed in wild-type mice. As increased GLUT4 translocation occurs with increased Akt phosphorylation [30], it is likely that the increased translocation of GLUT4 would also have facilitated an increased uptake of glucose in wild-type mice.

In summary, our results suggest that the changes in the expression level of key insulin signaling proteins precede the significant increase in brain $A\beta_{42}$ level in AβPPsw/PS1ΔE9 mice. This early perturbation in brain insulin signaling was accompanied by reduced glucose and insulin content. Although the exact mechanism underlining this connection remains unclear, our results imply an early role for insulin signaling impairment leading to amyloid accumulation in AβPPsw/PS1ΔE9 mice.

ACKNOWLEDGMENTS

This work was supported by grants to BSW from the National Medical Research Council (NMRC/1148/2008) and the Biomedical Research Council (BMRC/05/1/21/19/389 & 05/1/21/19/401). L.M.C. was supported by a graduate scholarship from Singapore Ministry of Education.

Authors' disclosures available online (http://www.j-alz.com/disclosures/view.php?id=1127).

REFERENCES

[1] Mattson MP (2004) Pathways towards and away from Alzheimer's disease. *Nature* **430**, 631-639.

[2] Schubert D (2005) Glucose metabolism and Alzheimer's disease. *Ageing Res Rev* **4**, 240-257.

[3] Jagust W, Gitcho A, Sun F, Kuczynski B, Mungas D, Haan M (2006) Brain imaging evidence of preclinical Alzheimer's disease in normal aging. *Ann Neurol* **59**, 673-681.

[4] Nordberg A, Rinne JO, Kadir A, Langstrom B (2010) The use of PET in Alzheimer disease. *Nat Rev Neurol* **6**, 78-87.

[5] Mosconi L, De Santi S, Li J, Tsui WH, Li Y, Boppana M, Laska E, Rusinek H, de Leon MJ (2008) Hippocampal hypometabolism predicts cognitive decline from normal aging. *Neurobiol Aging* **29**, 676-692.

[6] Hartmann J, Kiewert C, Klein J (2010) Neurotransmitters and energy metabolites in amyloid-bearing APP(SWE)xPSEN1dE9 Mouse Brain. *J Pharmacol Exp Ther* **332**, 364-370.

[7] Hsiao KK, Borchelt DR, Olson K, Johannsdottir R, Kitt C, Yunis W, Xu S, Eckman C, Younkin S, Price D et al. (1995) Age-related CNS disorder and early death in transgenic FVB/N mice overexpressing Alzheimer amyloid precursor proteins. *Neuron* **15**, 1203-1218.

[8] Sadowski M, Pankiewicz J, Scholtzova H, Ji Y, Quartermain D, Jensen CH, Duff K, Nixon RA, Gruen RJ, Wisniewski T (2004) Amyloid-beta deposition is associated with decreased hippocampal glucose metabolism and spatial memory impairment in APP/PS1 mice. *J Neuropathol Exp Neurol* **63**, 418-428.

[9] Hauptmann S, Scherping I, Drose S, Brandt U, Schulz KL, Jendrach M, Leuner K, Eckert A, Muller WE (2009) Mitochondrial dysfunction: An early event in Alzheimer pathology accumulates with age in AD transgenic mice. *Neurobiol Aging* **30**, 1574-1586.

[10] Hooijmans CR, Graven C, Dederen PJ, Tanila H, van Groen T, Kiliaan AJ (2007) Amyloid beta deposition is related to decreased glucose transporter-1 levels and hippocampal atrophy in brains of aged APP/PS1 mice. *Brain Res* **1181**, 93-103.

[11] Bevan P (2001) Insulin signalling. *J Cell Sci* **114**, 1429-1430.

[12] Cohen E, Dillin A (2008) The insulin paradox: Aging, proteotoxicity and neurodegeneration. *Nat Rev Neurosci* **9**, 759-767.

[13] Haan MN (2006) Therapy Insight: Type 2 diabetes mellitus and the risk of late-onset Alzheimer's disease. *Nat Clin Pract Neurol* **2**, 159-166.

[14] Irie F, Fitzpatrick AL, Lopez OL, Kuller LH, Peila R, Newman AB, Launer LJ (2008) Enhanced risk for Alzheimer disease in persons with type 2 diabetes and APOE epsilon4: The Cardiovascular Health Study Cognition Study. *Arch Neurol* **65**, 89-93.

[15] Taubes G (2003) Insulin insults may spur Alzheimer's disease. *Science* **301**, 40-41.

[16] Schrijvers EM, Witteman JC, Sijbrands EJ, Hofman A, Koudstaal PJ, Breteler MM (2010) Insulin metabolism and the risk of Alzheimer disease: The Rotterdam Study. *Neurology* **75**, 1982-1987.

[17] Liu Y, Liu F, Grundke-Iqbal I, Iqbal K, Gong CX (2011) Deficient brain insulin signalling pathway in Alzheimer's disease and diabetes. *J Pathol* **225**, 54-62.

[18] Deng Y, Li B, Liu Y, Iqbal K, Grundke-Iqbal I, Gong CX (2009) Dysregulation of insulin signaling, glucose transporters, O-GlcNAcylation, and phosphorylation of tau and neurofilaments in the brain: Implication for Alzheimer's disease. *Am J Pathol* **175**, 2089-2098.

[19] Moloney AM, Griffin RJ, Timmons S, O'Connor R, Ravid R, O'Neill C (2010) Defects in IGF-1 receptor, insulin receptor and IRS-1/2 in Alzheimer's disease indicate possible resistance to IGF-1 and insulin signalling. *Neurobiol Aging* **31**, 224-243.

[20] Steen E, Terry BM, Rivera EJ, Cannon JL, Neely TR, Tavares R, Xu XJ, Wands JR, de la Monte SM (2005) Impaired insulin and insulin-like growth factor expression and signaling mechanisms in Alzheimer's disease–is this type 3 diabetes? *J Alzheimers Dis* **7**, 63-80.

[21] Jankowsky JL, Fadale DJ, Anderson J, Xu GM, Gonzales V, Jenkins NA, Copeland NG, Lee MK, Younkin LH, Wagner SL, Younkin SG, Borchelt DR (2004) Mutant presenilins specifically elevate the levels of the 42 residue beta-amyloid peptide *in vivo*: Evidence for augmentation of a 42-specific gamma secretase. *Hum Mol Genet* **13**, 159-170.

[22] Goh AX, Li C, Sy MS, Wong BS (2007) Altered prion protein glycosylation in the aging mouse brain. *J Neurochem* **100**, 841-854.

[23] Ashe KH, Zahs KR (2010) Probing the biology of Alzheimer's disease in mice. *Neuron* **66**, 631-645.

[24] Jankowsky JL, Xu G, Fromholt D, Gonzales V, Borchelt DR (2003) Environmental enrichment exacerbates amyloid plaque formation in a transgenic mouse model of Alzheimer disease. *J Neuropathol Exp Neurol* **62**, 1220-1227.

[25] Wood IS, Trayhurn P (2003) Glucose transporters (GLUT and SGLT): Expanded families of sugar transport proteins. *Br J Nutr* **89**, 3-9.

[26] Prapong T, Buss J, Hsu WH, Heine P, West Greenlee H, Uemura E (2002) Amyloid beta-peptide decreases neuronal glucose uptake despite causing increase in GLUT3 mRNA transcription and GLUT3 translocation to the plasma membrane. *Exp Neurol* **174**, 253-258.

[27] Ma QL, Yang F, Rosario ER, Ubeda OJ, Beech W, Gant DJ, Chen PP, Hudspeth B, Chen C, Zhao Y, Vinters HV, Frautschy SA, Cole GM (2009) Beta-amyloid oligomers induce phosphorylation of tau and inactivation of insulin receptor substrate via c-Jun N-terminal kinase signaling: Suppression by omega-3 fatty acids and curcumin. *J Neurosci* **29**, 9078-9089.

[28] Zhao L, Teter B, Morihara T, Lim GP, Ambegaokar SS, Ubeda OJ, Frautschy SA, Cole GM (2004) Insulin-degrading enzyme as a downstream target of insulin receptor signaling cascade: Implications for Alzheimer's disease intervention. *J Neurosci* **24**, 11120-11126.

[29] Ueki K, Fruman DA, Yballe CM, Fasshauer M, Klein J, Asano T, Cantley LC, Kahn CR (2003) Positive and negative roles of p85 alpha and p85 beta regulatory subunits of phosphoinositide 3-kinase in insulin signaling. *J Biol Chem* **278**, 48453-48466.

[30] Ducluzeau PH, Fletcher LM, Welsh GI, Tavare JM (2002) Functional consequence of targeting protein kinase B/Akt to GLUT4 vesicles. *J Cell Sci* **115**, 2857-2866.